Am J Transl Res 2021;13(3):1085-1108
www.ajtr.org /ISSN:1943-8141/AJTR0119035

Original Article

Potential targets identified in adenoid cystic carcinoma point out new directions for further research

Zhenan Liu[1], Jian Gao[2], Yihui Yang[3], Huaqiang Zhao[1], Chuan Ma[1], Tingting Yu[4]

[1]Department of Oral and Maxillofacial Surgery, School and Hospital of Stomatology, Cheeloo College of Medicine, Shandong University & Shandong Key Laboratory of Oral Tissue Regeneration & Shandong Engineering Laboratory for Dental Materials and Oral Tissue Regeneration, Jinan, China; [2]Department of Stomatology, Xintai Hospital of Traditional Chinese Medicine, Taian, China; [3]Department of Orthodontics, School and Hospital of Stomatology, Cheeloo College of Medicine, Shandong University & Shandong Key Laboratory of Oral Tissue Regeneration & Shandong Engineering Laboratory for Dental Materials and Oral Tissue Regeneration, Jinan, China; [4]Department of Oral and Maxillofacial Surgery, Jinan Stomatological Hospital, Jinan, China

Received July 27, 2020; Accepted December 8, 2020; Epub March 15, 2021; Published March 30, 2021

Abstract: Adenoid cystic carcinoma (AdCC) of the head and neck originates from salivary glands, with high risks of recurrence and metastasis that account for the poor prognosis of patients. The purpose of this research was to identify key genes related to AdCC for further investigation of their diagnostic and prognostic significance. In our study, the AdCC sample datasets GSE36820, GSE59702 and GSE88804 from the Gene Expression Omnibus (GEO) database were used to explore the abnormal coexpression of genes in AdCC compared with their expression in normal tissue. A total of 115 DEGs were obtained by screening with GEO2R and FunRich software. According to functional annotation analysis using Enrichr, these DEGs were mainly enriched in the SOX2, AR, SMAD and MAPK signaling pathways. A protein-protein network of the DEGs was established by the Search Tool for the Retrieval of Interacting Genes (STRING) and annotated through the WEB-based Gene SeT AnaLysis Toolkit (WebGestalt) and was shown to be enriched with proteins involved in cardiac muscle cell proliferation and extracellular matrix organization. A Kyoto Encyclopedia of Genes and Genomes (KEGG) analysis revealed that ITGA9, LAMB1 and BAMBI were associated with the PI3K-Akt and TGF-β pathways. Furthermore, 36 potential target miRNAs were identified by the OncomiR and miRNA Pathway Dictionary Database (miRPathDB). In conclusion, SLC22A3, FOXP2, Cdc42EP3, COL27A1, DUSP1 and HSPB8 played critical roles according to the enrichment analysis; ITGA9, LAMB1 and BAMBI were involved in significant pathways according to the KEGG analysis; ST3Gal4 is a pivotal component of the PPI network of all the DEGs obtained; SPARC, COL4A2 and PRELP were highly related to multiple malignancies in pan-cancer research; hsa-miR-29-3p, hsa-miR-132-3p and hsa-miR-708-5p were potential regulators in AdCC. The involved pathways, biological processes and miRNAs have been shown to play significant roles in the genesis, growth, invasion and metastasis of AdCC. In this study, these identified DEGs were considered to have a potential influence on AdCC but have not been studied in this disease. The analysis results promote our understanding of the molecular mechanisms and biological processes of AdCC, which might be useful for targeted therapy or diagnosis.

Keywords: Adenoid cystic carcinoma, bioinformatics, differentially expressed genes, miRNA

Introduction

Adenoid cystic carcinoma (AdCC), previously called “cylindroma”, has been classified as a highly malignant tumor and is reportedly derived from the reserve cells of the intercalated ducts in salivary glands [1, 2]. AdCC is most frequently located in major and minor salivary glands, accounting for approximately 1% of total head and neck cancers and approximately 20% of malignant tumors of the salivary gland [3]. With the characteristics of perineural invasion, an infiltrating growth pattern and a relatively high probability of distant metastasis, the prognosis of AdCC tends to be unfavorable [4]. Although a series of therapy technologies has been used for the treatment of AdCC, including surgical resection and postoperative chemoradiotherapy, tumor recurrence and hematogenous metastasis cannot be prevented due to

the growth traits of AdCC [5-7]. To find a treat this malignant salivary gland tumor and improve the prognosis of patients with AdCC, many studies have been performed [8-10]. It has been proven that several significant factors, such as the MYB proto-oncogene, transmembrane receptor NOTCH1, nerve growth factor (NGF) and vascular endothelial growth factor (VEGF), have profound effects on the cell differentiation, proliferation, invasion and metastasis of AdCC [8-10]. Some of these findings are applied to the treatment of AdCC; however, obvious restrictions impede its application, and improvement seems unlikely [11]. Therefore, more work on the molecular and pathological mechanisms is urgently needed.

In recent years, with the wide-spread application of bioinformatics, online databases and analysis tools have been swiftly improved, driving considerable research based on data analysis [12-16]. Microarray analysis, based on an emerging technology for detecting simultaneously expressed genes, is being adopted in a large variety of biological studies, and many analysis results are available online by uploading to database websites [17]. For AdCC, researchers utilize microarrays and other kinds of technologies to determine the critical factors that regulate the proliferation, recurrence and metastasis of tumors, which are remarkable but insufficient, and numerous difficulties remain unresolved in the treatment of AdCC [18-20]. In conclusion, it is worthwhile to explore sample data of AdCC to determine the unknown molecular mechanism of this disease.

In this research, we scanned all available data of patients with AdCC from the Gene Expression Omnibus (GEO) database and collected the GSE36820, GSE59702 and GSE88804 online datasets. The abnormally expressed genes of two datasets were filtered by GEO2R, an online analysis tool. FunRich version 3.1.3 software was used to compare the aberrantly expressed genes of the two groups and identify co-upregulated/co-downregulated genes, which were identified as differentially expressed genes (DEGs) [21]. DEGs were generally analyzed in two ways. On the one hand, DEGs were regarded as an integral gene group and were analyzed through network databases and tools, including Genotype-Tissue Expression (GTEx), Search Tool for the Retrieval of Interacting Genes (STRING), Cytoscape and Enrichr. On the other hand, each DEG was analyzed by the Human Protein Atlas (HPA), Gene Expression Profiling Interactive Analysis (GEPIA) and GeneCards. By exploring DEG functions, interactions, related pathways and expression in other kinds of malignancies, it is possible to reveal the potential diagnostic factors, prognostic criteria and targets for therapies of AdCC.

Materials and methods

Sample data from the GEO database

The strategy for searching the GEO database (https://www.ncbi.nlm.nih.gov/geo/) was ["carcinoma, adenoid cystic" [MeSH Terms] OR adenoid cystic carcinoma [All Fields]]. All datasets shown were examined carefully, and only 3 datasets qualified for our research, namely, GSE36820, GSE59702 and GSE88804, which can be tracked online (https://www.ncbi.nlm.nih.gov/geo/query/acc.cgi?acc=GSE36820/, https://www.ncbi.nlm.nih.gov/geo/query/acc.cgi?acc=GSE59702/, and https://www.ncbi.nlm.nih.gov/geo/query/acc.cgi?acc=GSE88804/). Forty-one samples in the 3 datasets were selected, including 16 ACC surgical samples, 7 ACC xenografts in mouse hosts and 18 samples of normal salivary glands (NSGs). All samples originated from the oral cavity and were available for online analysis.

Gene expression analysis and DEG identification

The selected samples from each dataset were compared by GEO2R, an R-based web application13. Analysis was performed by "Analyze with GEO2R" option. Then, 3 series of all the abnormally expressed genes were created and downloaded from the GEO database for comparison. DEGs in the 3 datasets were identified based on the cut-off criteria (*P*-value ≤0.05, adjusted *P*-value ≤0.05 and LogIFCl ≥1.6). After identification, the 3 groups of DEGs were uploaded into FUNRICH (version 3.1.3) [21]. In the initial interface of this software, the "Upload datasets" option was used for collecting and comparing DEGs in the 3 datasets. Through this software, two Venn diagrams were created demonstrating the co-upregulated and co-downregulated DEGs. The volcano plot graph based on the expression levels of the DEGs

was designed by R Software (version 3.6.3, https://www.r-project.org/) [22].

Enrichment analysis of the DEGs with Enrichr

A recently released website, Enrichr (http://amp.pharm.mssm.edu/Enrichr), which includes various databases, such as Gene Ontology (GO) and Kyoto Encyclopedia of Genes and Genomes (KEGG), has become an efficient enrichment analysis tool [23]. All gene symbols of the DEGs were entered into the text box on the homepage of Enrichr and submitted. For the Enrichr analysis results, the results from the ChIP enrichment analysis (ChEA) of the transcription section, kinase enrichment analysis (KEA) of the pathway section, GEO of the crowd section and GO of the ontology section were screened and collected [24-26].

Protein-protein interaction network and hub gene identification

The Search Tool for the Retrieval of Interacting Genes (STRING, https://string-db.org) is a suitable online tool for protein-protein-interaction (PPI) analysis [15]. All DEGs were uploaded, and the minimum required interaction score was set to 0.15. With the recognition of DEGs, the PPI network data were generated and downloaded from the "exports" menu. Furthermore, the PPI network was uploaded to Cytoscape version 3.7.2 [14]. The plug-in stringApp version 1.5.1 and cytoHubba version 0.1 were installed and used for the PPI analysis. StringApp was used to reestablish and simplify the PPI network; thus, we divided the complicated network into 3 major functional subnetworks. CytoHubba was used for the determination of hub genes. Before the calculation was performed, the number of hub genes was set to 20 and ranked by the "MCC" method.

Enrichment analysis of 3 functional groups of DEGs with WebGestalt

DEGs in the 3 subnetworks were examined by WebGestalt. WebGestalt (WEB-based Gene SeT AnaLysis Toolkit, http://www.webgestalt.org/), another powerful online analysis website, is used by biological researchers from a variety of fields [27]. In addition to uploading DEGs, we chose "geneontology" and "biological process" for the "Functional Database" option. For "Reference Set", genome protein-coding was selected. The enrichment plot diagram was reestablished by the "ggplot" package in R Software.

Single gene function analysis

Hub genes and the other DEGs were searched by GeneCards (https://www.genecards.org/), and the general functions were listed in the summary section of this website. The top 50 expressed genes of NSGs were compared with those in other human organs by Genotype-Tissue Expression (GTEx, http://www.gtexportal.org/) through the "Top Expressed Genes" of the "Expression" menu [28]. Then, a "cancer vs. normal" analysis of the DEGs was performed with the Oncomine database (http://www.oncomine.org), using the filters "Cancer vs. Normal Analysis" and each of the gene symbols separately [29]. The significant DEGs were filtered and compared against previous research. In addition, the degree of the expression and the function of the DEGs in other kinds of malignancies and normal tissues were summarized. The function of the DEGs was examined with KEGG (Kyoto Encyclopedia of Genes and Genomes, https://www.genome.jp/keg/) to determine the relevant pathways enriched with DEGs [12]. The pathway search entry of KEGG is located in the "KEGG PATHWAY" option in the "Data-oriented entry points" section.

Establishment of the miRNA-mRNA regulatory network and KEGG pathway analysis of miRNAs

MiRNAs are short RNAs of 19-25 nucleotides that influence the expression of target genes that are involved in functional signaling pathways. We scanned all of the DEGs and obtained 6 DEGs (Cdc42EP3; SLC22A3; COL27A1; DUSP1; ITGA9; and PRELP) for consideration. In our study, OncomiR (http://www.oncomir.org/), an online database for exploring the functions of miRNAs in major types of cancer, was used to analyze related miRNAs [30]. Potential miRNA-target pairs were predicted through "Search for miRNA-Target Correlation" in the homepage of OncomiR. After predicting the miRNAs, we performed KEGG pathway analysis through the miRNA Pathway Dictionary Database (miRPathDB, https://mpd.bioinf.uni-sb.de/) [31]. Evidence was selected through the "Experimental" and "Predicted" options

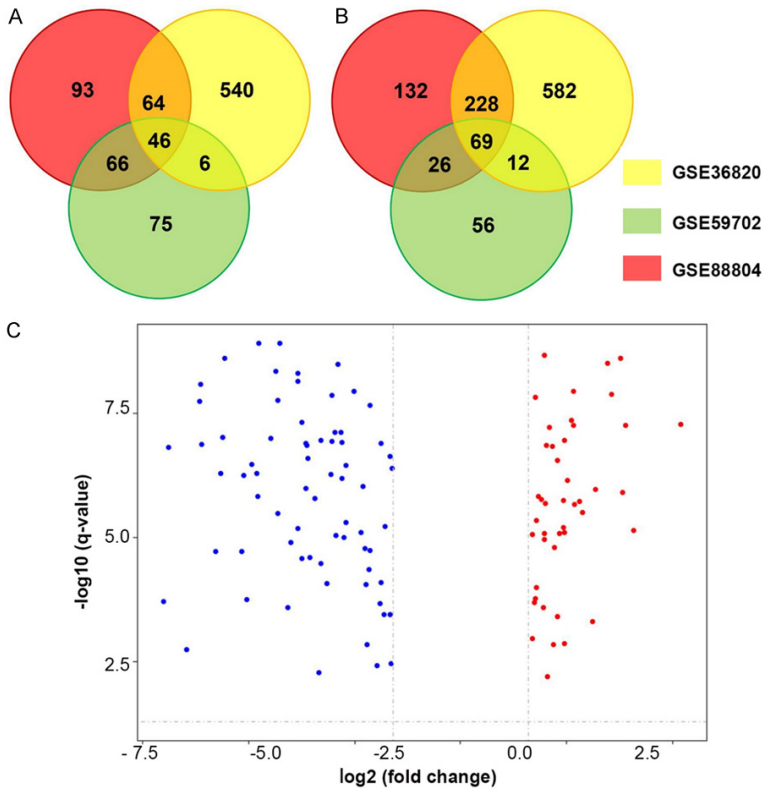

Figure 1. Identification of DEGs from GSE36820, GSE59702 and GSE88804 datasets. A, B. Venn diagram of co-upregulated DEGs and co-downregulated DEGs analyzed on differentially expressed genes from the three AdCC datasets. C. Volcano plot of all DEGs. Red plots represent up-regulated DEGs and blue plots represent down-regulated DEGs. *P*-value ≤0.05, adjusted *P*-value ≤0.05, LogIFCI ≥1.6

separately. Finally, 2 heat maps were created and downloaded.

Results

Gene expression analysis and DEG identification

We successfully collected valuable abnormally expressed genes from the GEO database for further research. The raw data from the GSE36820, GSE59702 and GSE88804 datasets were analyzed and downloaded from the GEO website. All abnormally expressed genes were filtered by the cut-off criteria (*P*-value ≤0.05, adjusted *P*-value ≤0.05 and LogIFCI ≥1.6). Based on the first filtration, 658 genes in GSE36820, 195 genes in GSE59702 and 271 genes in GSE88804 were upregulated and selected, and 893 genes in GSE36820, 165 genes in GSE59702 and 457 genes in GSE88804 were downregulated and selected. All the selected genes were analyzed by FunRich software, and unidentified genes were eliminated; 46 co-upregulated genes and 69 co-downregulated genes were finally adopted as DEGs (**Figure 1**). All the selected DEGs are shown in **Table 1**.

Enrichr analysis of the DEGs

The results generated by Enrichr revealed a variety of information from different databases. All the DEGs were uploaded into Enrichr to find a series of integral biological processes. **Figure 2** shows the most relevant enriched terms and pathways as revealed by ChEA, KEA and GEO analysis. The ChEA demonstrated that the 115 DEGs were significantly enriched in the SOX2, AR, SMAD4, GATA1 and SUZ12 signaling pathways (**Figure 2A**). The KEA analysis revealed highly correlated kinases, such as MAP2K1, MAPK3, MAPK4 and IGF1R (**Figure 2B**). In terms of disease perturbations identified in the GEO database, the DEGs were most significantly matched with the AdCC samples, followed by Barrett's esophagus samples, Sjogen's syndrome samples, hereditary gingival fibromatosis samples and other samples of other types of malignancies (**Figure 2C**, **2D**). **Figure 2E** is a diagram summarizing **Figure 2A**, **2B** and shows the DEGs associated with each enriched term.

Establishment of the PPI network and hub gene identification

In addition to hub genes, potential functional DEG subnetworks were found in the PPI network. The STRING database was utilized to construct a PPI network with 115 DEGs. As shown in **Figure 3A**, 115 nodes (genes) and 507 edges (interactions) were combined to create the PPI network of DEGs (PPI enrichment *p*-value < 1.0e-16). After setting a high required interaction score, 71 of 115 DEGs were filtered out,

Table 1. Differentially expressed genes (DEGs) of 3 GEO datasets

DEGs	Gene symbol
Up-regulated	MFGE8, ART3, EFHD1, ITGA9, COL27A1, ZNF711, FABP7, LAMB1, VCAN, SLC35F3, BCL2, EN1, ZNF286, FAT1, NTRK3, OBP2B, IL17RB, ST3GAL4, MFAP2, FGFR1, MICAL3, CDK6, FNDC1, BMPR1B, SPARC, PRAME, CDC42EP3, NOTCH1, COL4A2, VTCN1, AADAT, GABRP, PDE9A, DAPK1, ZFHX4, PRELP, PRLR, SERPINE2, EY2, ELAVL2, BAMBI, SCRG1, STMN1, COL9A1, ABCA13, HORMAD1
Down-regulated	MGLL, KAT2B, AQP3, FAM3B, TMEM45B, FOXP2, FAM3D, CD36, ELL2, SCNN1A, MAOB, SIDT1, SQRDL, HSPB8, FUT2, FABP4, FAM107B, KLK11, SLC22A3, ATP1B1, PAX9, DEFB1, DEPTOR, FBP1, PARM1, ALDH1A1, MUC15, DUSP1, MEIS2, RRAGD, ABI3BP, FAM46C, CRISP3, STEAP4, ADH1C, SH3BGRL2, SLAMF7, HBB, PTGS2, SERPINB1, SLC26A9, FAM129A, DPP4, TESC, TMPRSS11E, IGKC, GPR160, PIP, ALDH1L2, LYZ, STATH, DMBT1, WIF1, SMR3A, LCN2, LPO, GGTA1P, TSPAN8, PIGR, TMC5, JCHAIN, OPRPN, MUC7, ZG16B, HTN1, ODAM, BPIFA2, TCN1, PRB3

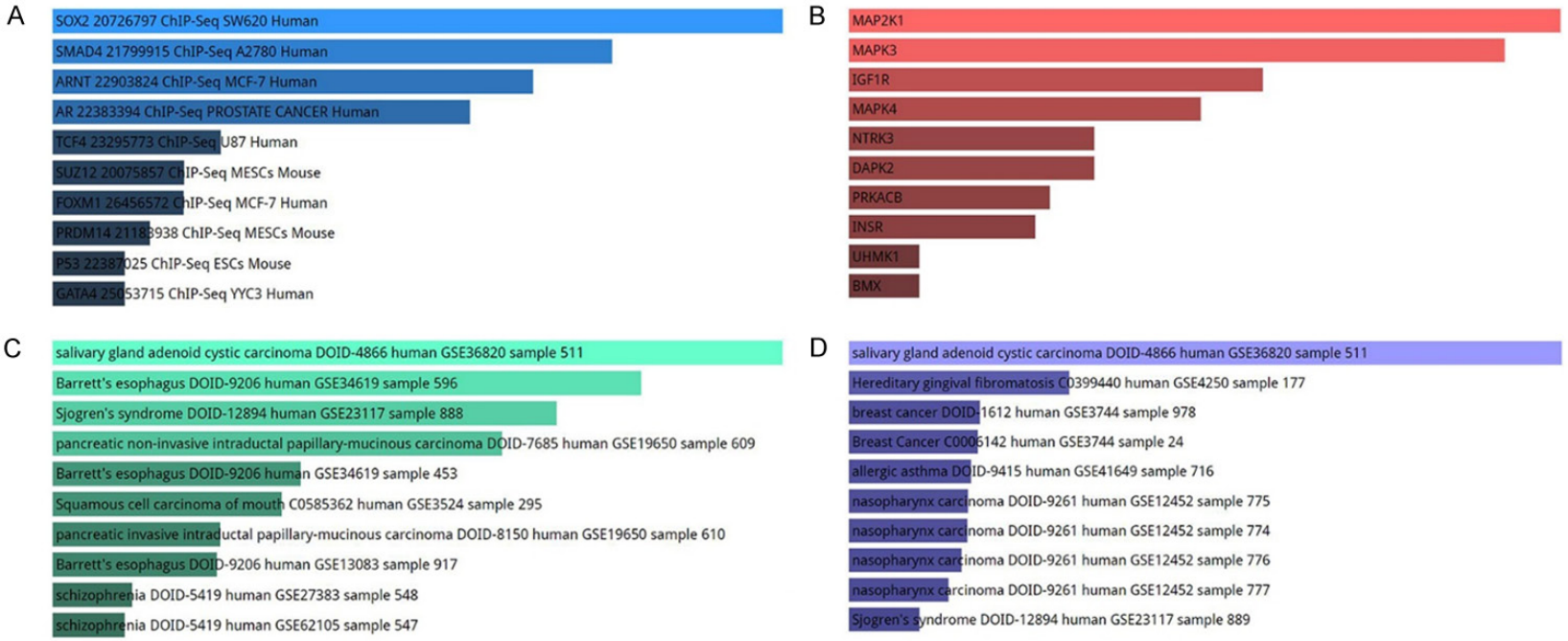

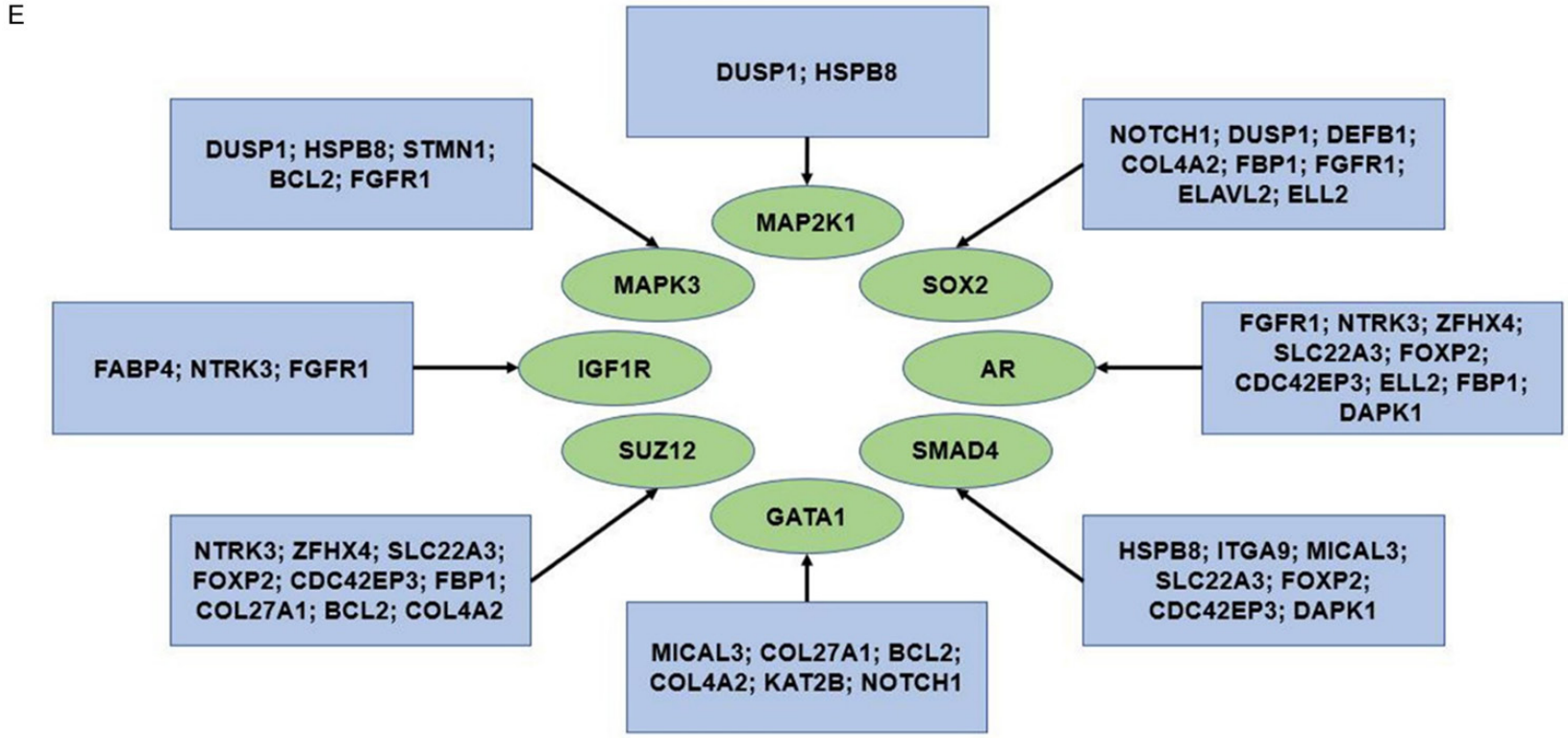

Figure 2. Enrichment analysis for DEGs. A. TOP 10 enriched terms of ChIP Enrichment Analysis (ChEA). B. Kinase Enrichment Analysis (KEA). C, D. Disease perturbations from GEO. E. An overview of Enriched term connections between ChEA and KEA. Enrichment *p*-value < 0.05.

and a simplified PPI network based on the residual 44 DEGs was established (**Figure 3B**). Three separate PPI networks were generated, with several key genes playing significant roles in each (NOTCH1, MUC7, ST3Gal4 and PRELP). To continue further study, the three PPI networks were defined as three DEG groups. The top 20 hub genes were identified by calculation with the cytoHubba plug-in (**Figure 3C**). It is clear that the top 1-10 hub genes and 11-20 hub genes clustered. Red represents the top 1-10 hub genes, and blue represents the top 11-20 hub genes. The members in each DEG group are listed in **Table 2**.

DEG group enrichment analysis

The GO analysis revealed DEG functional groups in various biological processes. As shown in **Figure 3B**, three major DEG subset PPI networks were established. **Figure 4** shows the enriched terms of the three groups of DEGs. WebGestalt was used to reveal the slim summary of the GO enrichment analysis for these three groups of DEGs. Notably, group 1 DEGs were highly related to the positive regulation of cardiac muscle cell proliferation and triglyceride catabolic processes (**Figure 4B**). Group 2 DEGs were involved in the antimicrobial humoral response and defense response to bacteria. For group 3 DEGs, the top 2 enriched terms were extracellular matrix organization and extracellular structure organization (**Figure 4C**). The enrichment plot diagram was created in R software based on the results from WebGestalt, showing the 6 most significant GO terms among the 3 groups of DEGs (**Figure 4D**). **Table 3** lists all the GO terms and related gene members in each group for each function.

Single gene function analysis by GTEx and Oncomine

There were obvious differences among the expression levels of selected DEGs in different kinds of tumors. From the first analysis, we took all of the top 20 hub genes and two significant genes (ST3Gal4 and PRELP) from the PPI network into consideration. An in-depth exploration of the 22 DEGs was carried out. **Figure 5A** reveals the top 50 expressed genes in the NSGs compared with other normal human organs. Among the DEGs, PIGR, CRISP3, PIP, MUC7, BPIFB2 and LYZ were downregulated genes but highly expressed in normal salivary glands. All 22 DEGs were analyzed with the Oncomine database, and the least significant analysis results were screened out (**Figure 5B**). **Figure 5B** shows the "cancer vs. normal tissue" comparison results for several genes were remarkably upregulated or downregulated in different kinds of cancer. SPARC, COL4A2, SEPRINE2 and LAMB1 were all highly expressed in the brain and CNS cancer, gastric cancer, head and neck cancer and lymphoma. PIGR and CRISP3 were downregulated in head and neck cancer. For ST3Gal4, the expression level was significantly decreased in colorectal cancer and esophageal cancer. The expression level of PRELP was reduced in breast cancer, colorectal cancer, head and neck cancer, liver cancer, lung cancer and sarcoma.

Pathways with upregulated DEGs according to the KEGG analysis

Several DEGs were involved in 2 significant pathways according to the KEGG analysis. KEGG was employed to analyze all the upregulated DEGs to identify potential pathways that were critical for the progression, therapy and diagnosis of AdCC. After eliminating the genes that were researched or not sufficiently relevant, LAMB1, ITGA9 and BAMBI were ultimately determined from the KEGG analysis. **Figure 6** demonstrates the PI3K-Akt and TGF-β signaling pathways and their interaction with LAMB1, ITGA9 and BAMBI. As shown in **Figure 6A**, LAMB1 (from ECM proteins) interacted with ITGA9 (from ITGAs), regulating the function of the PI3K-Akt signaling pathway. **Figure 6B** shows that BAMBI plays a critical role in suppressing the TGF-β signaling pathway by inhibiting the BMPR, TGF-βR and Activin-R mechanisms.

MiRNA-mRNA regulatory network and KEGG pathway analysis

The potential miRNAs that might target DEGs and their related pathways were predicted. OncomiR was used to predict the miRNAs targeted to DEGs. After excluding the DEGs that have been studied in AdCC and were relatively less connected with miRNAs, Cdc42EP3, SLC22A3, COL27A1, DUSP1, ITGA9 and PRELP were selected for analysis. As shown in **Figure 7A**, 36 miRNAs were predicted to be potential suppressors of the target DEGs. **Figure 7B** is the heatmap that demonstrates the KEGG

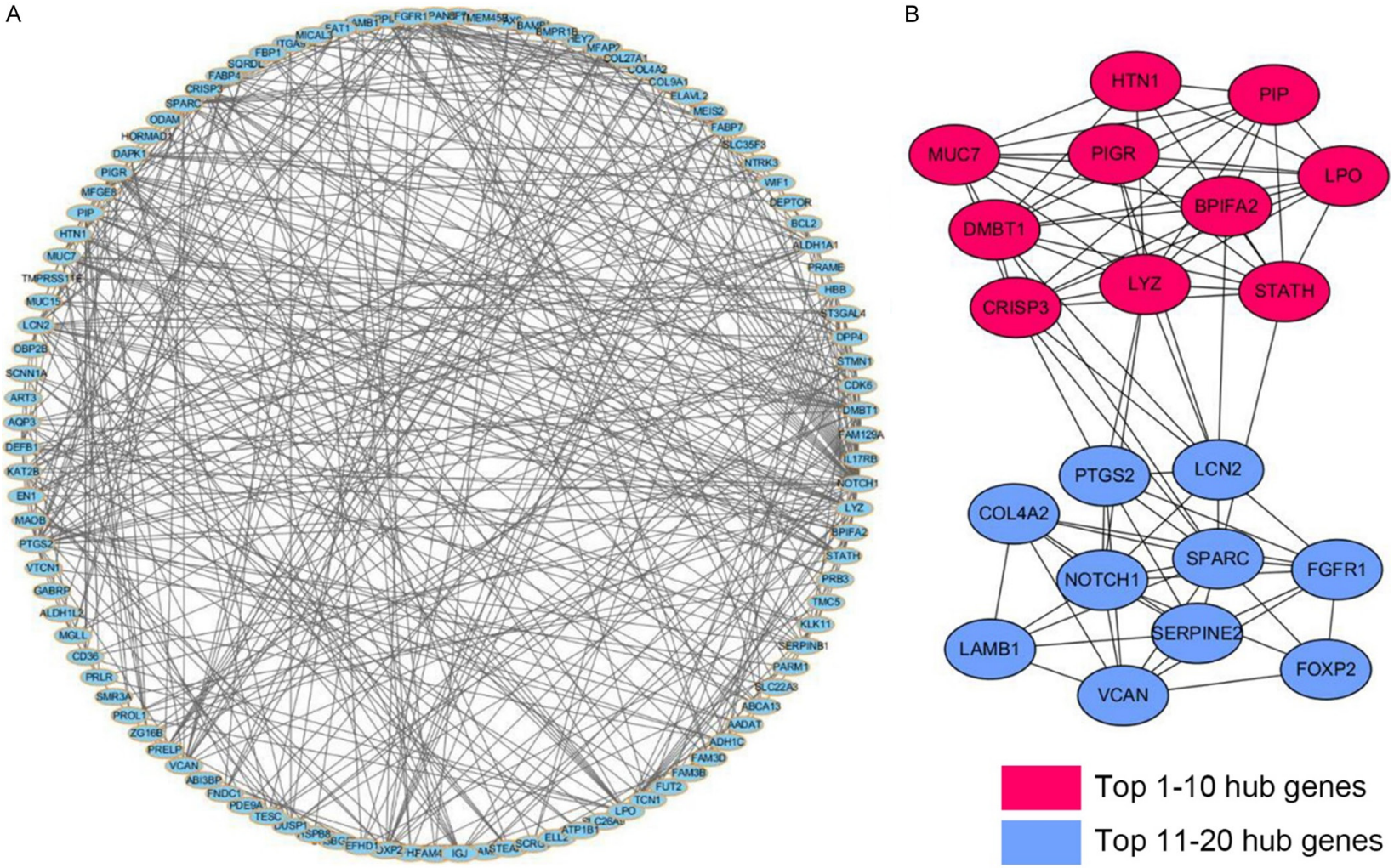
A
B
HTN1
PIP
MUC7
PIGR
LPO
BPIFA2
DMBT1
LYZ
STATH
CRISP3
PTGS2
LCN2
COL4A2
SPARC
FGFR1
NOTCH1
SERPINE2
LAMB1
FOXP2
VCAN
Top 1-10 hub genes
Top 11-20 hub genes

C

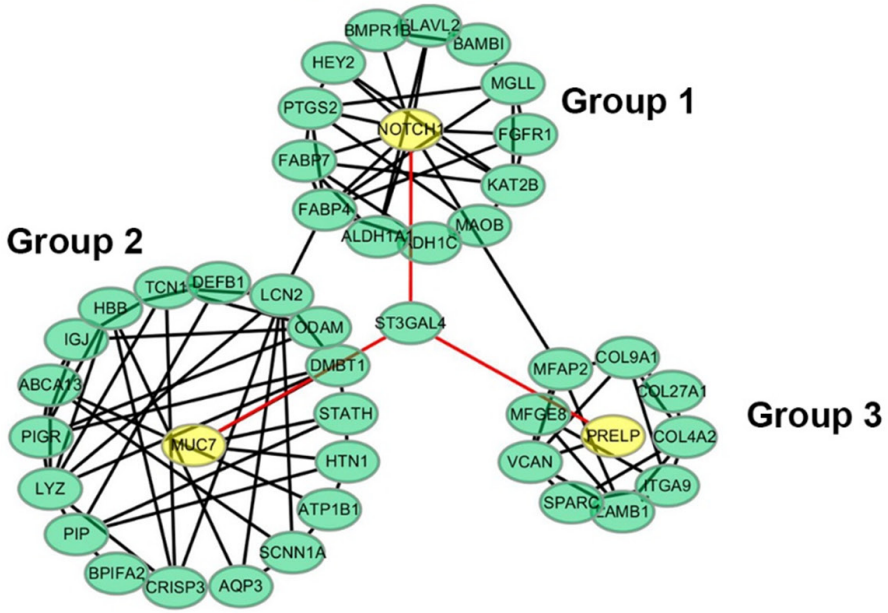

Figure 3. PPI network and hub gene identification. A. PPI network was established by all 115 DEGs. B. 71 relatively low connection confidence DEGs were eliminated and a simplified PPI network was built. C. Top 20 hub genes and the PPI network of them. PPI enrichment *p*-value < 1.0e-16.

Table 2. Gene members of 3 DEG groups analyzed by STRING

Group	Gene members
1	MAOB, PTGS2, HEY2, BMPR1B, BAMBI, ALDH1A1, NOTCH1, FABP7, ADH1C, FABP4, FGFR1, MGLL, KAT2B
2	LCN2, LYZ, ABCA13, IGJ, TCN1, ODAM, HBB, PIGR, DEFB1, PIP, STATH, IFA2, HTN1, CRISP3, ATP1B1, AQP3, SCNN1A, DMBT1, MUC7
3	MFAP2, MFGE8, ITGA9, SPARC, COL4A2, COL27A1, COL9A1, VCAN, LAMB1, PRELP

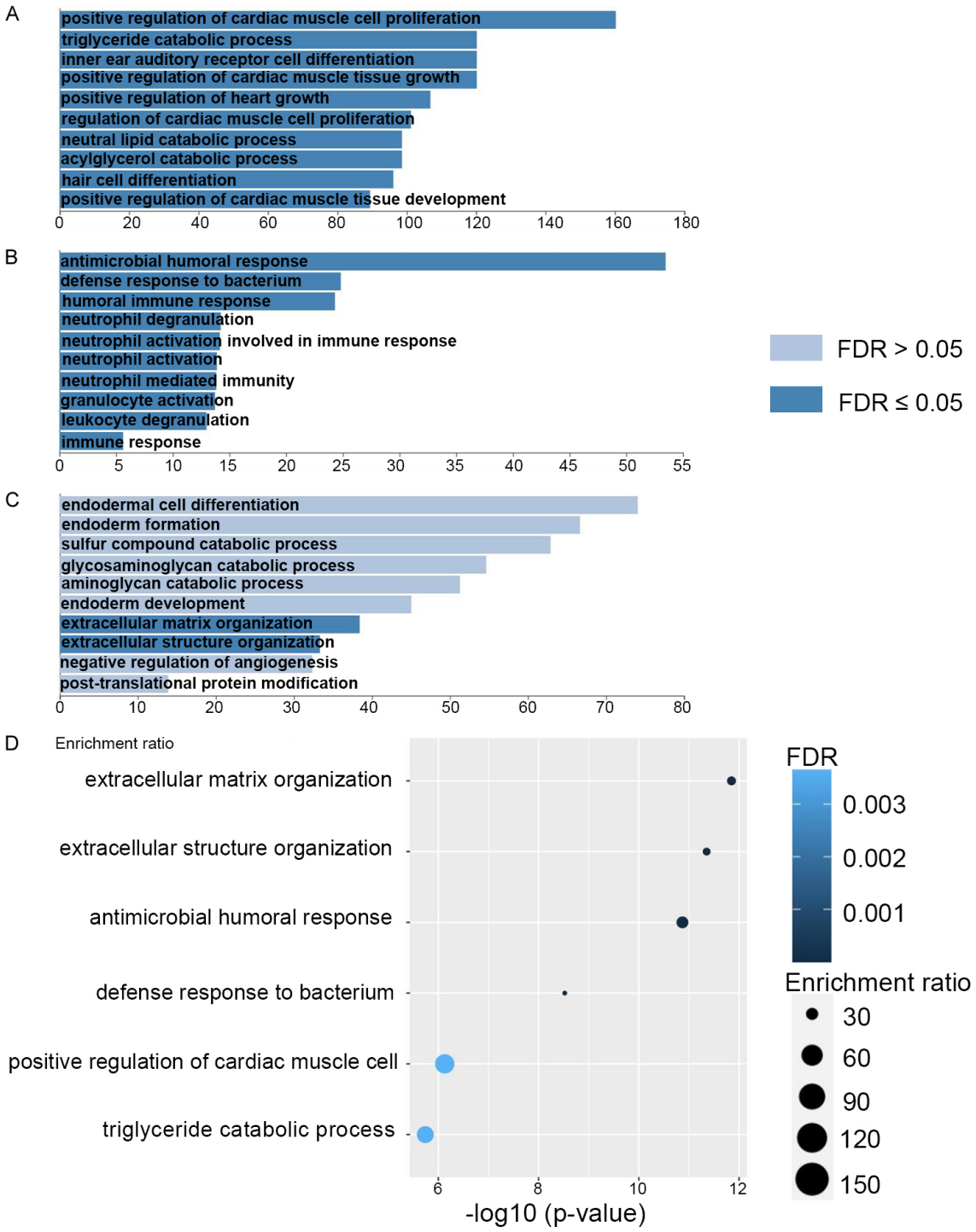

Figure 4. GO enrichment analysis by WebGestalt. A-C. GO enriched term analysis for 3 groups of DEGs. D. Enrichment plot diagram of GO analysis, processed by R software version 3.6.3. GO enrichment *p*-value < 0.05.

pathway associated with miRNAs based on previous experimental data, which reveals that the focal adhesion, PI3K-Akt and VEGF signaling pathways are highly relevant to the predicted miRNAs. **Figure 7C** is a predictive result of the miRNA-involved KEGG pathway analysis. Apart from focal adhesion and the PI3K-Akt signaling pathway, the TGF-β, MAPK and ErbB pathways, which have been proven to play significant roles in AdCC, are speculated to be highly associated

Table 3. Gene ontology (GO) analysis for 3 groups of DEGs

Gene group	Term/gene function	*P*-value	Involved gene member
1	GO:0060045/positive regulation of cardiac muscle cell proliferation	7.44E-07	HEY2; NOTCH1; FGFR1
	GO:0019433/triglyceride catabolic process	1.82E-06	FABP7; FABP4; MGLL
2	GO:0019730/antimicrobial humoral response	1.35E-11	LCN2; LYZ; DEFB1; BPIFA2; HTN1; DMBT1; MUC7
	GO:0042742/defense response to bacterium	3.00E-09	LCN2; LYZ; DEFB1; STATH; BPIFA2; HTN1; DMBT1
3	GO:0030198/extracellular matrix organization	1.42E-12	MFAP2; ITGA9; SPARC; COL4A2; COL27A1; COL9A1; VCAN; LAMB1
	GO:0043062/extracellular structure organization	4.44E-12	MFAP2; ITGA9; SPARC; COL4A2; COL27A1; COL9A1; VCAN; LAMB


A
TPM
0.0
6.9
61
4.0e+2
3.8e+3
3.0e+4
SAA1
DEFB1
AZGP1
PIGR
CRISP3
ZG16B
PIP
FDCSP
MUC7
BPIFB2
KRT19
SLPI
LYZ
IGKC
IGKJ1
IGHA1
IGKJ2
IGKJ4
IGHA2
JCHAIN
IGLC2
IGLC1
IGKJ3
IGKJ5
APOD
MTATP6P1
FTL
ACTB
TMSB10
RPL10
RPLP1
RPS18
RPL13A
RPS11
RPS12
EEF1A1
ACTG1
RPL3
RPS2
RPLP0
EEF2
RPS6
RPL9
RPL5
EEF1G
RPL8
RPS27
RPS16
RPS25
RPL19
Minor Salivary Gland
Muscle - Skeletal
Testis
Heart - Left Ventricle
Heart - Atrial Appendage
Adrenal Gland
Colon - Sigmoid
Artery - Tibial
Esophagus - Muscularis
Cells - Cultured fibroblasts
Brain - Cerebellum
Brain - Cerebellar Hemisphere
Brain - Spinal cord (cervical c-1)
Brain - Substantia nigra
Brain - Cortex
Brain - Frontal Cortex (BA9)
Brain - Anterior cingulate cortex (BA24)
Brain - Nucleus accumbens (basal ganglia)
Brain - Putamen (basal ganglia)
Brain - Caudate (basal ganglia)
Brain - Amygdala
Brain - Hypothalamus
Cells - Hippocampus
Whole Blood
Cells - EBV-transformed lymphocytes
Spleen
Stomach
Lung
Small Intestine - Terminal Ileum
Colon - Transverse
Prostate
Breast - Mammary Tissue
Skin - Sun Exposed (Lower leg)
Skin - Not Sun Exposed (Suprapubic)
Liver
Pancreas
Kidney - Medulla
Kidney - Cortex
Vagina
Esophagus - Mucosa
Fallopian Tube
Cervix - Endocervix
Cervix - Ectocervix
Nerve - Tibial
Adipose - Subcutaneous
Adipose - Visceral (Omentum)
Artery - Coronary
Artery - Aorta
Pituitary
Bladder
Thyroid
Uterus
Ovary

B

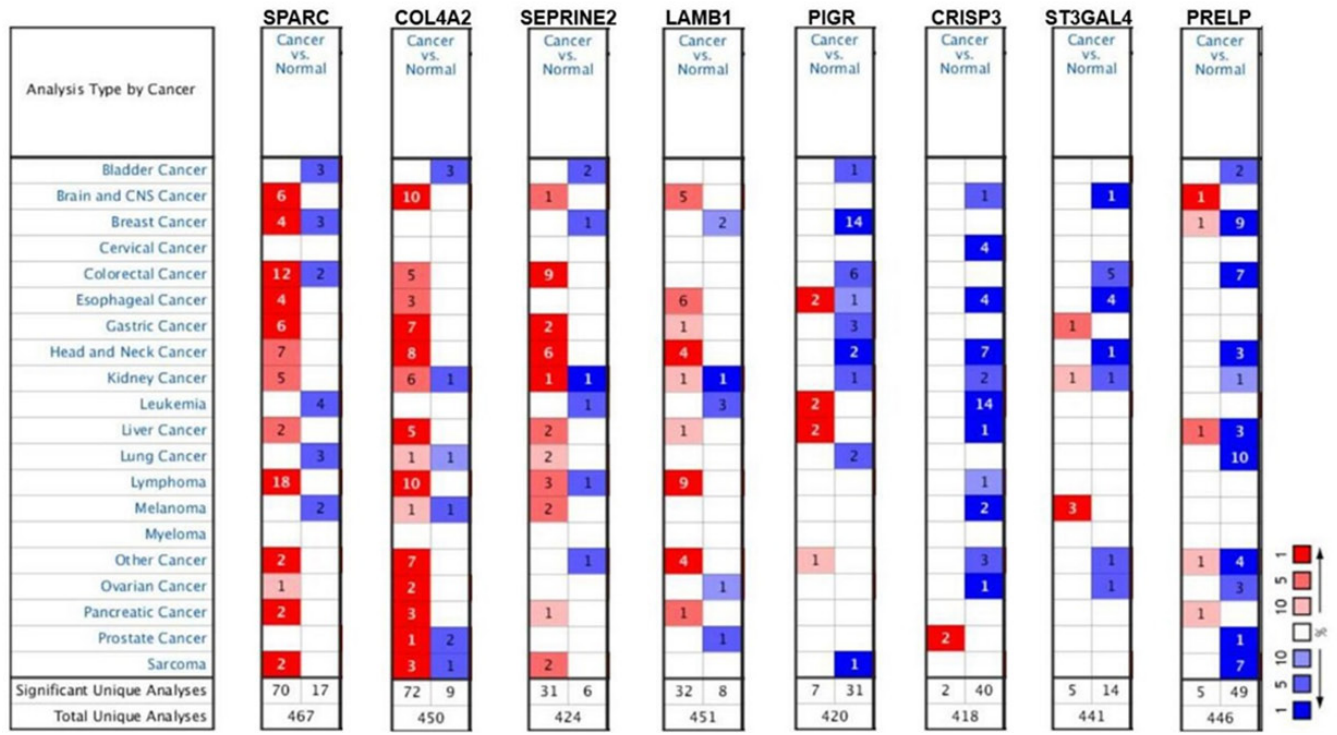

Figure 5. GTEx and Oncomine database analysis results. A. Top 50 expressed genes of normal salivary glands from GTEx. B. The expression level of SPARC, COL4A2, SEPRINE2, LAMB1, PIGR, CRISP3, ST3GAL4 and PRELP in different types of cancer. Gene expression *p*-value < 0.05.

A

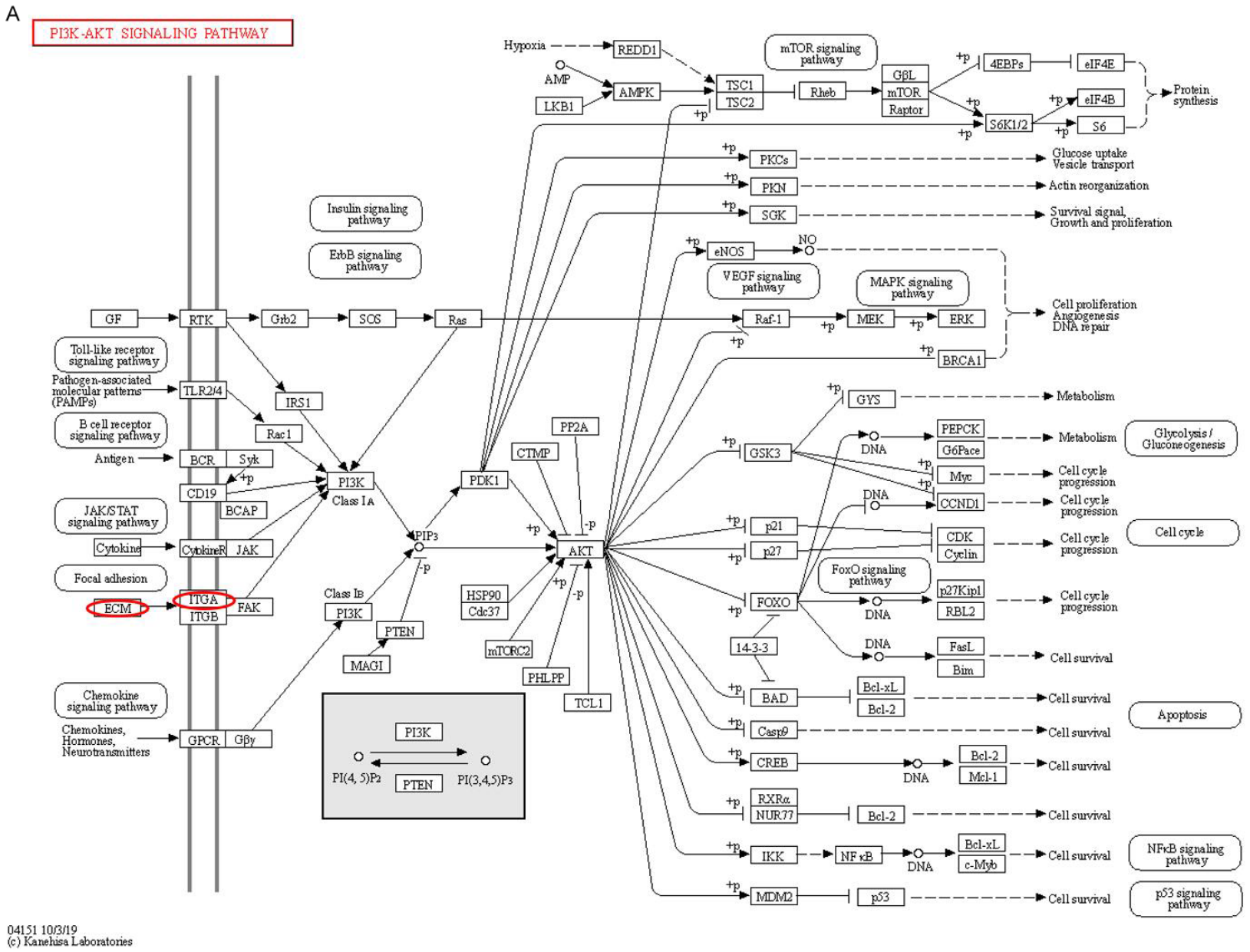
PI3K-AKT SIGNALING PATHWAY
Hypoxia
REDD1
AMP
AMPK
LKB1
mTOR signaling pathway
TSC1
TSC2
Rheb
GβL
mTOR
Raptor
4EBPs
eIF4E
eIF4B
S6K1/2
S6
Protein synthesis
PKCs
Glucose uptake
Vesicle transport
PKN
Actin reorganization
SGK
Survival signal,
Growth and proliferation
Insulin signaling pathway
ErbB signaling pathway
eNOS
NO
VEGF signaling pathway
MAPK signaling pathway
GF
RTK
Grb2
SOS
Ras
Raf-1
MEK
ERK
Cell proliferation
Angiogenesis
DNA repair
BRCA1
Toll-like receptor signaling pathway
Pathogen-associated molecular patterns (PAMPs)
TLR2/4
IRS1
B cell receptor signaling pathway
Antigen
BCR
Syk
Rac1
CD19
BCAP
PI3K
Class IA
PDK1
PP2A
CTMP
JAK/STAT signaling pathway
Cytokine
CytokineR
JAK
PIP3
AKT
Focal adhesion
ECM
ITGA
ITGB
FAK
Class IB
PI3K
PTEN
MAGI
HSP90
Cdc37
mTORC2
PHLPP
TCL1
Chemokine signaling pathway
Chemokines, Hormones, Neurotransmitters
GPCR
Gβγ
PI3K
PI(4, 5)P2
PTEN
PI(3,4,5)P3
GYS
Metabolism
GSK3
PEPCK
G6Pace
Metabolism
Glycolysis / Gluconeogenesis
DNA
Myc
Cell cycle progression
CCND1
Cell cycle progression
p21
p27
CDK
Cyclin
Cell cycle progression
Cell cycle
FoxO signaling pathway
FOXO
p27Kip1
RBL2
Cell cycle progression
14-3-3
FasL
Bim
Cell survival
BAD
Bcl-xL
Bcl-2
Cell survival
Apoptosis
Casp9
Cell survival
CREB
Bcl-2
Mcl-1
Cell survival
RXRα
NUR77
Bcl-2
Cell survival
IKK
NFκB
Bcl-xL
c-Myb
Cell survival
NFκB signaling pathway
MDM2
p53
Cell survival
p53 signaling pathway
04151 10/3/19
(c) Kanehisa Laboratories

B

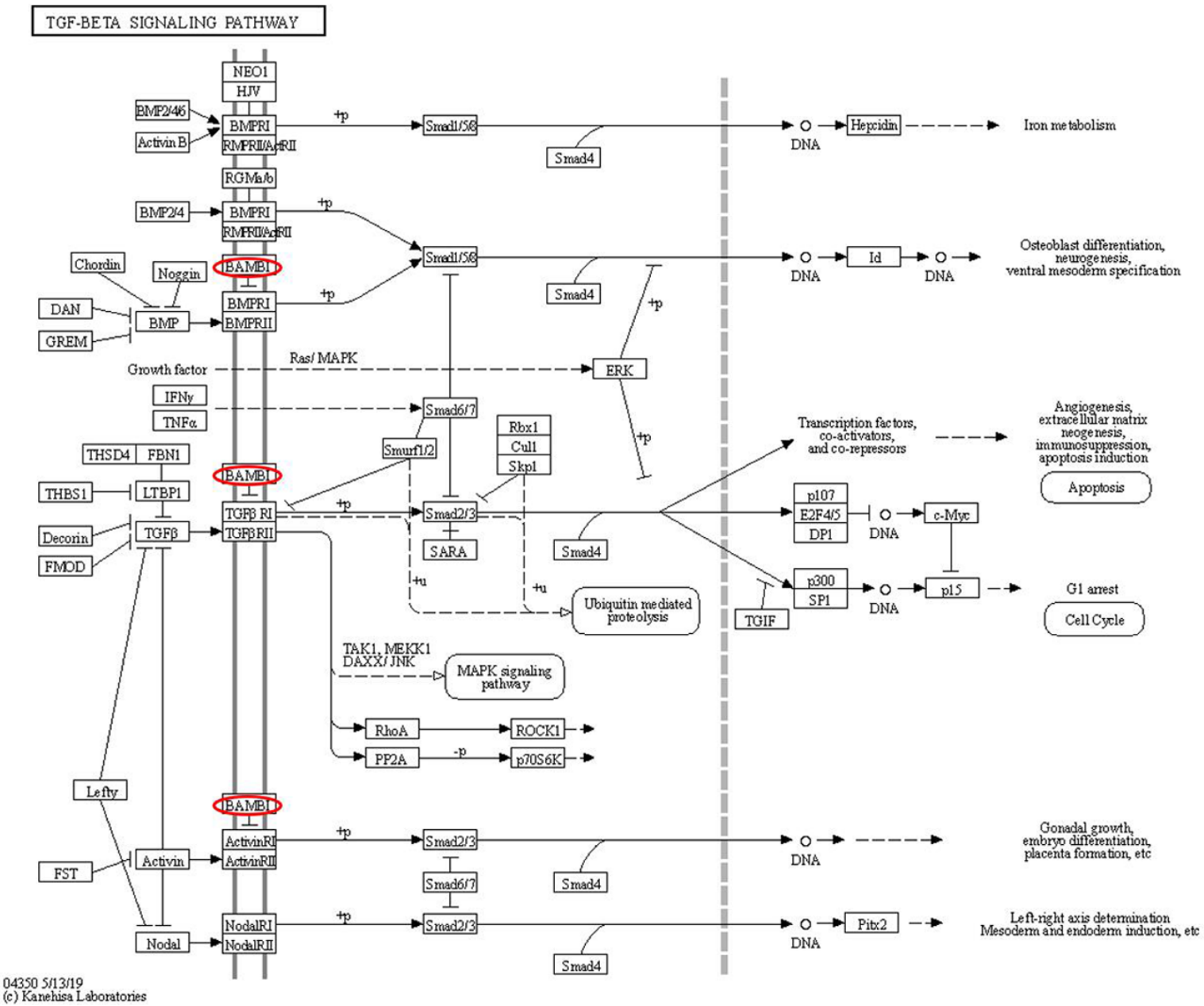
TGF-BETA SIGNALING PATHWAY
NEO1
HJV
BMP2/4/6
Activin B
BMPRI
RMPRII/ActRII
RGMa/b
BMP2/4
BMPRI
RMPRII/ActRII
Chordin
Noggin
BAMBI
DAN
GREM
BMP
BMPRI
BMPRII
Growth factor
Ras/ MAPK
ERK
IFNγ
TNFα
Smad6/7
Smurf1/2
Rbx1
Cul1
Skp1
THSD4
FBN1
THBS1
LTBP1
Decorin
FMOD
TGFβ
TGFβ RI
TGFβRII
Smad2/3
SARA
Smad4
Ubiquitin mediated proteolysis
TAK1, MEKK1
DAXX/ JNK
MAPK signaling pathway
RhoA
ROCK1
PP2A
p70S6K
Lefty
FST
Activin
ActivinRI
ActivinRII
Nodal
NodalRI
NodalRII
Smad1/5/8
Hepcidin
DNA
Iron metabolism
Id
Osteoblast differentiation, neurogenesis, ventral mesoderm specification
Transcription factors, co-activators, and co-repressors
Angiogenesis, extracellular matrix neogenesis, immunosuppression, apoptosis induction
Apoptosis
p107
E2F4/5
DP1
c-Myc
p300
SP1
TGIF
p15
G1 arrest
Cell Cycle
Gonadal growth, embryo differentiation, placenta formation, etc
Pitx2
Left-right axis determination
Mesoderm and endoderm induction, etc
04350 5/13/19
(c) Kanehisa Laboratories

Figure 6. KEGG pathway analysis on three up-regulated DEGs. A. The interaction network for PI3K-Akt signaling pathway associated with LAMB1 and ITGA9. B. The interaction network for TGF-β signaling pathway relevant to BAMBI. Analysis *p*-value < 0.05.

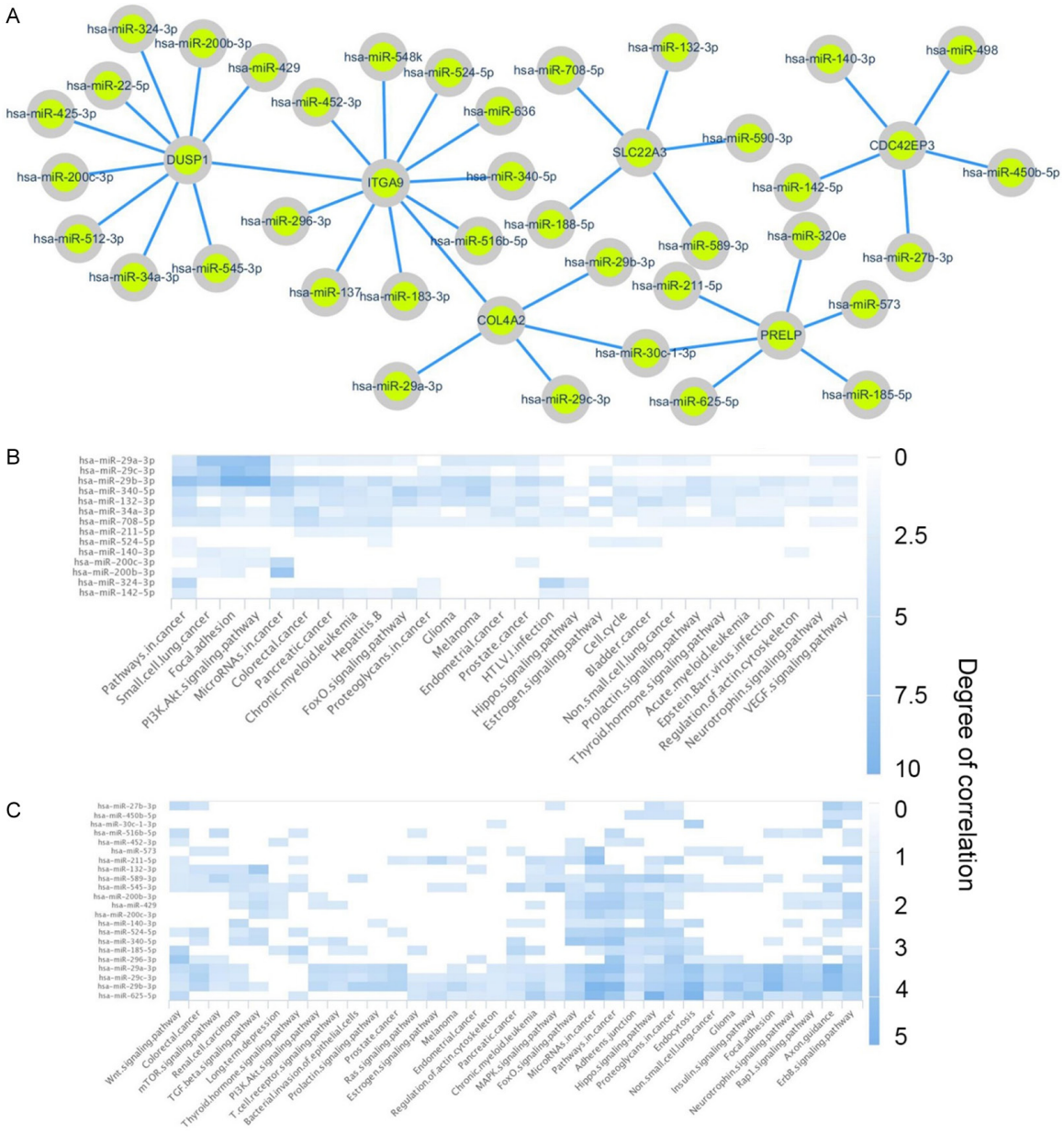

Figure 7. MiRNA-mRNA regulatory analysis from OncomiR and miRPathDB. A. OncomiR analysis for CDC42EP3, SLC22A3, COL27A1, DUSP1, ITGA9 and PRELP. B, C. Experimental and predictive KEGG pathway analysis from miRPathDB. MiRNA-mRNA analysis *p*-value < 0.05.

with miRNAs. **Table 4** includes all of the miRNA members related to the DEGs.

Discussion

AdCC of the head and neck develops as a consequence of pathological proliferation and differentiation of normal salivary gland cells. According to previous research, AdCC was once described as a highly troublesome tumor that is almost impossible to cure due to the high risk of invading adjacent soft tissue, bone and nerves [1-3]. Various types of therapy, including surgical resection, radiation and chemotherapeutic drugs, can be used to control the current

Table 4. MiRNA members of miRNA-mRNA analysis

Target gene	Related miRNAs
CDC42EP3	hsa-miR-142-5p; hsa-miR-450b-5p; hsa-miR-140-3p; hsa-miR-498; hsa-miR-27b-3p
SLC22A3	hsa-miR-708-5p; sa-miR-589-3p; hsa-miR-132-3p; hsa-miR-590-3p; hsa-miR-188-5p
DUSP1	hsa-miR-429; hsa-miR-200b-3p; hsa-miR-324-3p; hsa-miR-425-3p; hsa-miR-200c-3p; hsa-miR-34a-3p; hsa-miR-22-5p; hsa-miR-512-3p; hsa-miR-545-3p
ITGA9	hsa-miR-183-3p; hsa-miR-452-3p; hsa-miR-137; hsa-miR-548k; hsa-miR-340-5p; hsa-miR-524-5p; hsa-miR-516b-5p; hsa-miR-636; hsa-miR-296-3p
COL4A2	hsa-miR-29c-3p; hsa-miR-29a-3p; hsa-miR-30c-1-3p; hsa-miR-29b-3p
PRELP	hsa-miR-185-5p; hsa-miR-625-5p; hsa-miR-30c-1-3p; hsa-hmiR-573; hsa-miR-320e; hsa-miR-211-5p

disease but cannot prevent recurrence in the future [4, 5]. With the characteristics of a relatively slow growth velocity, high potential of perineural invasion, infiltration of contiguous tissue and high risk of hematogenous metastasis, the bioinformatics mechanisms of AdCC tend to be complicated. In light of the current situation in the research and treatment of AdCC, identifying potential biomarkers and studying their roles in the origination, progression and metastasis of AdCC are of great importance. Because medical researchers contributed to the GSE36820, GSE59702 and GSE88804 datasets, we could conduct our the bioinformatics analysis of AdCC [32, 33]. In their previous research, MYB was found to be a critical transcriptional regulator influencing the clinical outcomes of patients with AdCC. NOTCH1 and RUNX1 were also found to regulate a series of key ACC-associated genes.

We first scanned all of the datasets of AdCC in the GEO database. Only three datasets (GSE36820, GSE59702 and GSE88804) met the following conditions: 1. both AdCC samples and normal tissue samples were included, and 2. raw data were available for online gene expression analysis through R language. Then, we identified 115 DEGs in the data extracted from three datasets. According to ChIP enrichment analysis, these DEGs were mainly involved in androgen receptor (AR), SRY-box transcription factor (SOX2), SMAD family member 4 (SMAD4), GATA-binding protein 1 (GATA1) and Polycomb repressive complex 2 subunit (SUZ12). AR is confirmed to be critical for the homeostasis of bone and muscle, which makes it one of the most promising targets for functional drug discovery [34]. Beata et al. found the ectopic expression of AR in some AdCC cells, referring to the biological behavior of AdCC, and we speculated that AR might participate in the bone and muscle invasion of AdCC [35, 36]. The study results from Cao et al. showed that the deletion of SMAD4, a negative regulator of the TGF-β pathway, led to AdCC development in murine salivary glands [37, 38]. In our research, SLC22A3, FOXP2 and Cdc42EP3 were related to both AR and SMAD4. Although these 3 DEGs have not been subjected to any relevant AdCC biological research, many studies on other kinds of human cancer were found. SLC22A3 and FOXP2 are reported to promote invasion and metastasis in esophageal cancer, account for susceptibility to pancreatic cancer, influence the progression of colorectal cancer and associate with tumor microenvironmental factors [39-43]. Furthermore, Cdc42EP3 plays critical roles in cancer-associated fibroblasts, thus stimulating the adhesion of tumor cells [44]. Several types of cancer that we mention here originate in tissues with abundant adenocytes, which are similar to salivary glands, and further research on the 3 DEG groups is needed. In addition, SLC22A3 directly renders chemoresistant tumor cells as members of the solute carrier family, while FOXP2 upregulates the expression of p21, which affects the genesis of tumor cells, indicating the clinical significance of targeted therapy for both of these DEGs [45, 46]. The other 2 enriched genes, GATA1 and SUZ12, tend to be involved in the cell cycle and tumorigenesis of several solid tumors, including squamous cell carcinoma of the head and neck, and are both associated with COL27A1, a newly discovered fibrillar collagen gene [47-51]. As fibrillar collagens function in the genesis and progression of tumors, the function of COL27A1 in AdCC remains unknown. Referring to our aforementioned research, it is clear that COL27A1 and Cdc42EP3 are both associated with the emergence of cancer-related fibroblasts and the accumulation of collagen in cancer [44, 52]. Consequently, the prospect of studying the possibility and mechanism by which COL27A1 and Cdc42EP3 may lead to fibrotic accumulation in AdCC is obvious. Based on kinase enrichment analysis, DUSP1 and HSPB8 are both highly relevant to the MAPK family (MAP2K1 and MAPK3). MAPKs convert extracellular signals into diverse cellular responses, and some members (MAP2K1 and MAPK3) enhance the risk of recurrence and aggressive growth of certain malignancies [53-56]. Due to insufficient research on AdCC, we only found evidence on the function of DUSP1 and HSPB8 in patients with gastric and ovarian cancer, and they induce cancer cell migration and thus worsen the prognosis for patients [57-60]. Demonstrating the potential meanings in both the clinic and research, the mechanisms by which DUSP1 and HSPB8 regulate the biological process of AdCC through the MAPK pathway need to be examined.

We utilized STRING to analyze the interaction among DEGs and found 20 hub genes that might play a critical role in AdCC. Unexpectedly,

3 series of DEGs seemed to cluster independently, and we defined them as 3 isolated gene groups. Through functional annotation, group 1 was found to be highly related to the positive regulation of cardiac muscle cell proliferation (HEY2, NOTCH1, and FGFR1) and triglyceride catabolic processes (FABP7, FABP4, and MGLL). These two myocyte-related functions play unique roles in AdCC. Morphologically, AdCC is divided into 3 architectural patterns (tubular, cribriform and solid), and the first 2 types contain a variety of neoplastic myofibrocytes surrounding nests of AdCC cells [61]. According to previous study, HEY2 regulates smooth muscle cell proliferation and is associated with NOTCH signals, indicating the value of the research on HEY2 in AdCC [62]. On the other hand, members of the FABP family was regarded as reliable biomarkers for myocardial injury, and combined with the muscle-invasion characteristics of AdCC, FABP4 and FABP7 are potential indices for an AdCC diagnosis [1, 63]. Group 2 was significantly related to the defense response to bacteria (LCN2, LYZ, DEFB1, STATH, BPIFA2, HTN1, and DMBT1) and the humoral immune response (LCN2, LYZ, DEFB1, BPIFA2, HTN1, DMBT1, and MUC7). Referring to the results from GTEx, these DEGs were highly expressed in normal salivary glands and downregulated in AdCC samples, demonstrating that the salivation function in AdCC was abnormal and providing new directions for exploring disordered cell secretion during the progression of AdCC. Group 3, with the same related gene members (MFAP2, ITGA9, SPARC, COL4A2, COL27A1, COL9A1, VCAN, and LAMB1) were mainly involved in extracellular matrix organization and extracellular structure organization. Combined with the KEGG analysis, this finding indicates that ITGA9 and LAMB1 are important factors regulating the PI3K-Akt pathway via the responses between the cytomembrane and extracellular matrix (ECM). According to other research, the interactions between cells and the ECM play critical roles in the biological processes of AdCC, such as cell adhesion, cell contact and the expression of genes that lead to cell migration, proliferation and differentiation [64]. Another study demonstrated that ECM components can accumulate in intercellular spaces, generating the typical morphologic structures in AdCC [65]. Consequently, LAMB1 and ITGA9, as important members in and regulators of in the ECM, are worthy of in-depth exploration in the context of AdCC. In addition, the PI3K-Akt pathway is reported to promote the tumorigenesis and distant metastasis of AdCC, and it is activated by upstream signals from the cell membrane and ECM [66-68]. Speculatively, the relationships between ECM, PI3K-Akt and our newly discovered genes (ITGA9 and LAMB1) may drive the development of AdCC and should be studied in future research.

Apart from LAMB1 and ITGA9, BAMBI might be an important factor in AdCC that is involved in the TGF-β signaling pathway, the KEGG analysis revealed that BAMBI served as the inhibitor of BMPR, TGF-βR and activinR, thus suppressing the function of TGF-β via smad1/5/8 and smad2/3 downstream signals. Generally, the TGF-β signaling pathway acts as a double-edged sword in cancer, inhibiting the progression of early-stage cancer but promoting metastasis and invasion of late-stage cancer [69]. Although it has been revealed that the promotion of AdCC migration and invasion through the TGF-β1/Smad2 pathway in vitro, the other functions of TGF-β in AdCC remain unknown [70]. BAMBI is a TGF-β pseudoreceptor that inhibits the TGF-β signaling pathway and promotes macrophage proliferation and differentiation [71]. This explanation indicates the possibility of targeted therapy for AdCC aimed at BAMBI.

Intriguingly, we found that ST3Gal4 functioned as a connecter between the 3 groups of DEGs. As shown in research, ST3Gal4 belongs to the sialyltransferase family (ST), resulting in aberrant glycosylation of cancer cells through the sialylation function [72]. The abnormal sialylation of glycoproteins and glycolipids is related to immune escape, chemotherapeutic resistance and hematogenous dissemination, causing tumor metastasis [72]. However, few experiments have been performed on the function of ST3Gal4 and other ST members in tumors, including AdCC. Prospectively, research on the potential roles of ST3Gal4 in AdCC might accelerate its progression in targeted therapy. Prospectively, research on the potential roles of ST3Gal4 in AdCC might reveal novel approaches for studying and curing this disease, which is difficult to cure.

Analysis using the Oncomine database revealed the aberrant expression of several DEGs in dif-

ferent types of cancer (SPARC, COL4A2, SEPRINE2, PIGR, CRISP3, and PRELP). SPARC is a matricellular protein involved in bone formation, fibrosis and angiogenesis [73]. High levels of SPARC have been reported in glioblastoma, breast cancer, colorectal cancer and melanoma and are associated with tumor growth and progression [74, 75]. As the function of SPARC remains unclear and controversial, understanding how it works in AdCC might be useful. COL4A2 is a newly discovered collagen member that is highly expressed in a variety of cancers. In previous research, COL4A2 was associated with vascular injury causing cerebrovascular disease [76]. Whether COL4A2 is correlated with AdCC remains to be proven. PRELP is another collagen-related protein and plays significant roles in basement membrane and cartilage formation [77]. In our research, PRELP was downregulated in AdCC, breast cancer, colorectal cancer, lung cancer and other kinds of head and neck cancer. The deficiency of PRELP accounts for Hutchinson-Gilford progeria (HGP) and vascular diseases, indicating its potential involvement in collagen-related biological processes of AdCC [77, 78]. Because COL4A2 and PRELP are rarely studied in AdCC, a focus of AdCC research on these 2 DEGs is promising.

Moreover, the results of KEGG analysis on related miRNAs demonstrated that significant pathways in AdCC were affected by miRNAs such as the PI3K-Akt, VEGF, TGF-β, MAPK and ErbB pathways. In our study, the hsa-miR-29 family seems to have an important influence on focal adhesion and the PI3K-Akt signaling pathway. Referring to a previous study, the hsa-miR-29 regulation of fibrinogen production might promote the formation of basic structures of AdCC [79]. While the ErbB and VEGF signaling pathways are regarded as important indicators for poor overall survival in patients with AdCC, the involvement of miRNAs (hsa-miR-29-3p, hsa-miR-132-3p, and hsa-miR-708-5p) in our predicted results suggest their potential value in studies of AdCC [80, 81].

Unfortunately, the analysis results from cBioPortal (cBio Cancer Genomics Portal, https://www.cbioportal.org/) and GEPIA (Gene Expression Profiling Interactive Analysis, http://gepia.cancer-pku.cn/) were less significant than the other results [16, 82]. The deficiency in samples of AdCC in cBioPortal restricted our ability to obtain meaningful data on the overall survival status related to the DEGs. In addition, we could not perform gene expression analysis of AdCC through GEPIA due to the limitations on its classification protocol for cancer. The identification of the top 20 hub genes revealed a series of genes expressed in normal salivary glands, narrowing the analysis range through hub genes. We tried to obtain useful information from some other platforms (e.g., Human Protein Atlas) but failed, indicating the lack of current investigation into AdCC. As a highly malignant carcinoma, there is much work to be completed on AdCC, from diagnosis methods to advanced targeted therapy.

Conclusion

We performed a series of bioinformatics analyses on samples of AdCC and found several potential targets for future study. Generally, SLC22A3, FOXP2, Cdc42EP3, COL27A1, DUSP1, HSPB8, ITGA9, LAMB1, BAMBI, ST3Gal4, SPARC, COL4A2, PRELP, hsa-miR-29-3p, hsa-miR-132-3p and hsa-miR-708-5p were potential regulators in the biological processes of AdCC. However, further molecular biological research is required to explore the true value of the identified DEGs in the laboratory and clinical applications.

Acknowledgements

This work was supported by the Natural Science Foundation of Shandong Province (No. ZR2020MH190).

Disclosure of conflict of interest

None.

Address correspondence to: Chuan Ma, Hospital of Stomatology, Shandong University, No. 44-1 Wenhua Road West, Jinan 250012, China. Tel: +86-188-88308321; E-mail: machuan@sdu.edu.cn; Tingting Yu, Department of Oral and Maxillofacial Surgery, Jinan Stomatological Hospital, No. 101 Jingliu Road, Jinan 250001, China. Tel: +86-18553162116; E-mail: yutt8713@sina.com

References

[1] Ellington CL, Goodman M, Kono SA, Grist W, Wadsworth T, Chen AY, Owonikoko T, Ramalingam S, Shin DM, Khuri FR, Beitler JJ and Saba NF. Adenoid cystic carcinoma of the head and

neck: incidence and survival trends based on 1973-2007 surveillance, epidemiology, and end results data. Cancer 2012; 118: 4444-4451.
[2] Spiro RH, Huvos AG and Strong EW. Adenoid cystic carcinoma of salivary origin. A clinicopathologic study of 242 cases. Am J Surg 1974; 128: 512-520.
[3] Kokemueller H, Eckardt A, Brachvogel P and Hausamen JE. Adenoid cystic carcinoma of the head and neck-a 20 years experience. Int J Oral Max Surg 2004; 33: 25-31.
[4] Vander PV, Balm AJ, Hilgers FJ, Tan IB, Loftus-Coll BM, Keus RB and Hart AA. Prognostic factors for long term results of the treatment of patients with malignant submandibular gland tumors. Cancer 1999; 85: 2255-2264.
[5] Lloyd S, Yu JB, Wilson LD and Decker RH. Determinants and patterns of survival in adenoid cystic carcinoma of the head and neck, including an analysis of adjuvant radiation therapy. Am J Clin Oncol 2011; 34: 76-81.
[6] Vander PV, Hunt J, Bradley PJ, Haigentz MJ, Rinaldo A, Mendenhall WM, Suarez C, Silver C, Takes RP and Ferlito A. Recent trends in the management of minor salivary gland carcinoma. Head Neck 2014; 36: 444-455.
[7] Wong SJ, Karrison T, Hayes DN, Kies MS, Cullen KJ, Tanvetyanon T, Argiris A, Takebe N, Lim D, Saba NF, Worden FP, Gilbert J, Lenz HJ, Razak AR, Roberts JD, Vokes EE and Cohen EE. Phase II trial of dasatinib for recurrent or metastatic c-KIT expressing adenoid cystic carcinoma and for nonadenoid cystic malignant salivary tumors. Ann Oncol 2016; 27: 318-323.
[8] Drier Y, Cotton MJ, Williamson KE, Gillespie SM, Ryan RJ, Kluk MJ, Carey CD, Rodig SJ, Sholl LM, Afrogheh AH, Faquin WC, Queimado L, Qi J, Wick MJ, El-Naggar AK, Bradner JE, Moskaluk CA, Aster JC, Knoechel B and Bernstein BE. An oncogenic MYB feedback loop drives alternate cell fates in adenoid cystic carcinoma. Nat Genet 2016; 48: 265-272.
[9] Ferrarotto R, Mitani Y, Diao L, Guijarro I, Wang J, Zweidler-McKay P, Bell D, William WN, Glisson BS, Wick MJ, Kapoun AM, Patnaik A, Eckhardt G, Munster P, Faoro L, Dupont J, Lee JJ, Futreal A, El-Naggar AK and Heymach JV. ActivatingNOTCH1 mutations define a distinct subgroup of patients with adenoid cystic carcinoma who have poor prognosis, propensity to bone and liver metastasis, and potential responsiveness to notch1 inhibitors. J Clin Oncol 2017; 35: 352-360.
[10] Li H, Nong XL, Chen Q, Yang YP, Li JQ and Li YN. Nerve growth factor and vascular endothelial growth factor: retrospective analysis of 63 patients with salivary adenoid cystic carcinoma. Int J Oral Sci 2010; 2: 35-44.
[11] Laurie SA and Licitra L. Systemic therapy in the palliative management of advanced salivary gland cancers. J Clin Oncol 2006; 24: 2673-2678.
[12] Kanehisa M and Goto S. KEGG: kyoto encyclopedia of genes and genomes. Nucleic Acids Res 2000; 28: 27-30.
[13] Barrett T, Wilhite SE, Ledoux P, Evangelista C, Kim IF, Tomashevsky M, Marshall KA, Phillippy KH, Sherman PM, Holko M, Yefanov A, Lee H, Zhang N, Robertson CL, Serova N, Davis S and Soboleva A. NCBI GEO: archive for functional genomics data sets-update. Nucleic Acids Res 2012; 41: D991-D995.
[14] Shannon P. Cytoscape: a software environment for integrated models of biomolecular interaction networks. Genome Res 2003; 13: 2498-2504.
[15] Szklarczyk D, Gable AL, Lyon D, Junge A, Wyder S, Huerta-Cepas J, Simonovic M, Doncheva NT, Morris JH, Bork P, Jensen LJ and Mering CV. STRING v11: protein-protein association networks with increased coverage, supporting functional discovery in genome-wide experimental datasets. Nucleic Acids Res 2019; 47: D607-D613.
[16] Tang Z, Li C, Kang B, Gao G, Li C and Zhang Z. GEPIA: a web server for cancer and normal gene expression profiling and interactive analyses. Nucleic Acids Res 2017; 45: W98-W102.
[17] Quackenbush J. Microarray analysis and tumor classification. N Engl J Med 2006; 354: 2463-2472.
[18] Chen W, Liu B, Zhang X, Zhao X, Cao G, Dong Z and Zhang S. Identification of differentially expressed genes in salivary adenoid cystic carcinoma cells associated with metastasis. Arch Med Sci 2016; 12: 881-888.
[19] Morris LGT, Chandramohan R, West L, Zehir A, Chakravarty D, Pfister DG, Wong RJ, Lee NY, Sherman EJ, Baxi SS, Ganly I, Singh B, Shah JP, Shaha AR, Boyle JO, Patel SG, Roman BR, Barker CA, McBride SM, Chan TA, Dogan S, Hyman DM, Berger MF, Solit DB, Riaz N and Ho AL. The molecular landscape of recurrent and metastatic head and neck cancers. JAMA Oncol 2017; 3: 244.
[20] Ross JS, Gay LM, Wang K, Vergilio JA, Suh J, Ramkissoon S, Somerset H, Johnson JM, Russell J, Ali S, Schrock AB, Fabrizio D, Frampton G, Miller V, Stephens PJ, Elvin JA and Bowles DW. Comprehensive genomic profiles of metastatic and relapsed salivary gland carcinomas are associated with tumor type and reveal new routes to targeted therapies. Ann Oncol 2017; 28: 2539-2546.
[21] Pathan M, Keerthikumar S, Ang CS, Gangoda L, Quek CY, Williamson NA, Mouradov D, Sieber OM, Simpson RJ, Salim A, Bacic A, Hill AF, Stroud DA, Ryan MT, Agbinya JI, Mariadason

JM, Burgess AW and Mathivanan S. FunRich: an open access standalone functional enrichment and interaction network analysis tool. Proteomics 2015; 15: 2597-2601.
[22] Mente S and Kuhn M. The use of the R language for medicinal chemistry applications. Curr Top Med Chem 2012; 12: 1957-1964.
[23] Kuleshov MV, Jones MR, Rouillard AD, Fernandez NF, Duan Q, Wang Z, Koplev S, Jenkins SL, Jagodnik KM, Lachmann A, McDermott MG, Monteiro CD, Gundersen GW and Ma'Ayan A. Enrichr: a comprehensive gene set enrichment analysis web server 2016 update. Nucleic Acids Res 2016; 44: W90-W97.
[24] Gene Ontology Consortium. Gene Ontology Consortium: going forward. Nucleic Acids Res 2015; 43: D1049-D1056.
[25] Lachmann A and Ma'Ayan A. KEA: kinase enrichment analysis. Bioinformatics 2009; 25: 684-686.
[26] Lachmann A, Xu H, Krishnan J, Berger SI, Mazloom AR and Ma'Ayan A. ChEA: transcription factor regulation inferred from integrating genome-wide ChIP-X experiments. Bioinformatics 2010; 26: 2438-2444.
[27] Wang J, Vasaikar S, Shi Z, Greer M and Zhang B. WebGestalt 2017: a more comprehensive, powerful, flexible and interactive gene set enrichment analysis toolkit. Nucleic Acids Res 2017; 45: W130-W137.
[28] Ardlie KG, Deluca DS, Segre AV, Sullivan TJ, Young TR, Gelfand ET, Trowbridge CA, Maller JB, Tukiainen T, Lek M, Ward LD, Kheradpour P, Iriarte B, Meng Y, Palmer CD, Esko T, Winckler W, Hirschhorn JN, Kellis M, MacArthur DG, Getz G, Shabalin AA, Li G, Zhou YH, Nobel AB, Rusyn I, Wright FA, Lappalainen T, Ferreira PG, Ongen H, Rivas MA, Battle A, Mostafavi S, Monlong J, Sammeth M, Mele M, Reverter F, Goldmann JM, Koller D, Guigo R, McCarthy MI, Dermitzakis ET, Gamazon ER, Im HK, Konkashbaev A, Nicolae DL, Cox NJ, Flutre T, Wen X, Stephens M, Pritchard JK, Tu Z, Zhang B, Huang T, Long Q, Lin L, Yang J, Zhu J, Liu J, Brown A, Mestichelli B, Tidwell D, Lo E, Salvatore M, Shad S, Thomas JA, Lonsdale JT, Moser MT, Gillard BM, Karasik E, Ramsey K, Choi C, Foster BA, Syron J, Fleming J, Magazine H, Hasz R, Walters GD, Bridge JP, Miklos M, Sullivan S, Barker LK, Traino HM, Mosavel M, Siminoff LA, Valley DR, Rohrer DC, Jewell SD, Branton PA, Sobin LH, Barcus M, Qi L, McLean J, Hariharan P, Um KS, Wu S, Tabor D, Shive C, Smith AM, Buia SA, Undale AH, Robinson KL, Roche N, Valentino KM, Britton A, Burges R, Bradbury D, Hambright KW, Seleski J, Korzeniewski GE, Erickson K, Marcus Y, Tejada J, Taherian M, Lu C, Basile M, Mash DC, Volpi S, Struewing JP, Temple GF, Boyer J, Colantuoni D, Little R, Koester S, Carithers LJ, Moore HM, Guan P, Compton C, Sawyer SJ, Demchok JP, Vaught JB, Rabiner CA, Lockhart NC, Ardlie KG, Getz G, Wright FA, Kellis M, Volpi S and Dermitzakis ET. The Genotype-Tissue Expression (GTEx) pilot analysis: multitissue gene regulation in humans. Science 2015; 348: 648-660.
[29] Rhodes DR, Yu J, Shanker K, Deshpande N, Varambally R, Ghosh D, Barrette T, Pandey A and Chinnaiyan AM. ONCOMINE: a cancer microarray database and integrated data-mining platform1. Neoplasia 2004; 6: 1-6.
[30] Wong NW, Chen Y, Chen S and Wang X. OncomiR: an online resource for exploring pan-cancer microRNA dysregulation. Bioinformatics 2018; 34: 713-715.
[31] Backes C, Kehl T, Stöckel D, Fehlmann T, Schneider L, Meese E, Lenhof H and Keller A. miRPathDB: a new dictionary on microRNAs and target pathways. Nucleic Acids Res 2017; 45: D90-D96.
[32] Gao R, Cao C, Zhang M, Lopez M, Yan Y, Chen Z, Mitani Y, Zhang L, Zajac-Kaye M, Liu B, Wu L, Renne R, Baker HV, El-Naggar A and Kaye FJ. A unifying gene signature for adenoid cystic cancer identifies parallel MYB-dependent and MYB-independent therapeutic targets. Oncotarget 2014; 5: 12528-12542.
[33] Andersson MK, Afshari MK, Andrén Y, Wick MJ and Stenman G. Targeting the oncogenic transcriptional regulator MYB in adenoid cystic carcinoma by inhibition of IGF1R/AKT signaling. J Natl Cancer Inst 2017; 109.
[34] Fujii S and Kagechika H. Androgen receptor modulators: a review of recent patents and reports (2012-2018). Expert Opin Ther Pat 2019; 29: 439-453.
[35] Jagielska B, Sarnowska E, Rusetska N, Jancewicz I, Durzynska M, Kubala S, Chmielik E, Paul P, Rutkowski T, Sarnowski TJ and Siedlecki JA. Advanced adenoid cystic carcinoma (ACC) is featured by SWI/SNF chromatin remodeling complex aberrations. J Cancer Res Clin 2019; 145: 201-211.
[36] Gentile MS, Yip D, Liebsch NJ, Adams JA, Busse PM and Chan AW. Definitive proton beam therapy for adenoid cystic carcinoma of the nasopharynx involving the base of skull. Oral Oncol 2017; 65: 38-44.
[37] Cao Y, Liu H, Gao L, Lu L, Du L, Bai H, Li J, Said S, Wang X, Song J, Serkova N, Wei M, Xiao J and Lu S. Cooperation between pten and smad4 in murine salivary gland tumor formation and progression. Neoplasia 2018; 20: 764-774.
[38] Zhao M, Mishra L and Deng C. The role of TGF-β/SMAD4 signaling in cancer. Int J Biol Sci 2018; 14: 111-123.
[39] Cervenkova L, Vycital O, Bruha J, Rosendorf J, Palek R, Liska V, Daum O, Mohelnikova-Duchonova B and Soucek P. Protein expression of

ABCC2 and SLC22A3 associates with prognosis of pancreatic adenocarcinoma. Sci Rep 2019; 9: 19782.
[40] Fu L, Qin Y, Ming X, Zuo X, Diao Y, Zhang L, Ai J, Liu B, Huang T, Cao T, Tan B, Xiang D, Zeng C, Gong J, Zhang Q, Dong S, Chen J, Liu H, Wu J, Qi RZ, Xie D, Wang L and Guan X. RNA editing ofSLC22A3 drives early tumor invasion and metastasis in familial esophageal cancer. Proc Natl Acad Sci U S A 2017; 114: E4631-E4640.
[41] Ishaque N, Abba ML, Hauser C, Patil N, Paramasivam N, Huebschmann D, Leupold JH, Balasubramanian GP, Kleinheinz K, Toprak UH, Hutter B, Benner A, Shavinskaya A, Zhou C, Gu Z, Kerssemakers J, Marx A, Moniuszko M, Kozlowski M, Reszec J, Niklinski J, Eils J, Schlesner M, Eils R, Brors B and Allgayer H. Whole genome sequencing puts forward hypotheses on metastasis evolution and therapy in colorectal cancer. Nat Commun 2018; 9: 4782.
[42] Kim JH, Hwang J, Jung JH, Lee HJ, Lee DY and Kim SH. Molecular networks of FOXP family: dual biologic functions, interplay with other molecules and clinical implications in cancer progression. Mol Cancer 2019; 18: 180.
[43] Ren A, Sun S, Li S, Chen T, Shu Y, Du M and Zhu L. Genetic variants in SLC22A3 contribute to the susceptibility to colorectal cancer. Int J Cancer 2019; 145: 154-163.
[44] Calvo F, Ranftl R, Hooper S, Farrugia AJ, Moeendarbary E, Bruckbauer A, Batista F, Charras G and Sahai E. Cdc42EP3/BORG2 and septin network enables mechano-transduction and the emergence of cancer-associated fibroblasts. Cell Rep 2015; 13: 2699-2714.
[45] Kim J, Hwang J, Jung JH, Lee H, Lee DY and Kim S. Molecular networks of FOXP family: dual biologic functions, interplay with other molecules and clinical implications in cancer progression. Mol Cancer 2019; 18: 119-180.
[46] Shnitsar V, Eckardt R, Gupta S, Grottker J, Müller GA, Koepsell H, Burckhardt G and Hagos Y. Expression of human organic cation transporter 3 in kidney carcinoma cell lines increases chemosensitivity to melphalan, irinotecan, and vincristine. Cancer Res 2009; 69: 1494-1501.
[47] Andrieux LO, Fautrel A, Bessard A, Guillouzo A, Baffet G and Langouët S. GATA-1 is essential in EGF-mediated induction of nucleotide excision repair activity and ERCC1 expression through ERK2 in human hepatoma cells. Cancer Res 2007; 67: 2114-2123.
[48] Boidot R, Végran F, Jacob D, Chevrier S, Cadouot M, Feron O, Solary E and Lizard-Nacol S. The transcription factor GATA-1 is overexpressed in breast carcinomas and contributes to survivin upregulation via a promoter polymorphism. Oncogene 2010; 29: 2577-2584.
[49] Jenkins E, Moss J, Pace J and Bridgewater L. The new collagen gene contains SOX9-responsive enhancer elements. Matrix Biol 2005; 24: 177-184.
[50] Pace JM, Corrado M, Missero C and Byers PH. Identification, characterization and expression analysis of a new fibrillar collagen gene, COL27A1. Matrix Biol 2003; 22: 3-14.
[51] Peters I, Dubrowinskaja N, Tezval H, Kramer MW, von Klot CA, Hennenlotter J, Stenzl A, Scherer R, Kuczyk MA and Serth J. Decreased mRNA expression of GATA1 and GATA2 is associated with tumor aggressiveness and poor outcome in clear cell renal cell carcinoma. Target Oncol 2015; 10: 267-275.
[52] Li X, Shepard HM, Cowell JA, Zhao C, Osgood RJ, Rosengren S, Blouw B, Garrovillo SA, Pagel MD, Whatcott CJ, Han H, Von Hoff DD, Taverna DM, LaBarre MJ, Maneval DC and Thompson CB. Parallel accumulation of tumor hyaluronan, collagen, and other drivers of tumor progression. Clin Cancer Res 2018; 24: 4798-4807.
[53] Baba Y, Nosho K, Shima K, Meyerhardt JA, Chan AT, Engelman JA, Cantley LC, Loda M, Giovannucci E, Fuchs CS and Ogino S. Prognostic significance of AMP-activated protein kinase expression and modifying effect of MAPK3 1 in colorectal cancer. Br J Cancer 2010; 103: 1025-1033.
[54] Cargnello M and Roux PP. Activation and function of the MAPKs and their substrates, the MAPK-activated protein kinases. Microbiol Mol Biol Rev 2011; 75: 50-83.
[55] Jain AP, Patel K, Pinto S, Radhakrishnan A, Nanjappa V, Kumar M, Raja R, Patil AH, Kumari A, Manoharan M, Karunakaran C, Murugan S, Keshava Prasad TS, Chang X, Mathur PP, Kumar P, Gupta R, Gupta R, Khanna-Gupta A, Sidransky D, Chatterjee A and Gowda H. MAP2K1 is a potential therapeutic target in erlotinib resistant head and neck squamous cell carcinoma. Sci Rep 2019; 9: 18793.
[56] Nikolaev SI, Rimoldi D, Iseli C, Valsesia A, Robyr D, Gehrig C, Harshman K, Guipponi M, Bukach O, Zoete V, Michielin O, Muehlethaler K, Speiser D, Beckmann JS, Xenarios I, Halazonetis TD, Jongeneel CV, Stevenson BJ and Antonarakis SE. Exome sequencing identifies recurrent somatic MAP2K1 and MAP2K2 mutations in melanoma. Nat Genet 2012; 44: 133-139.
[57] Kang Y, Seok H, Jeong E, Kim Y, Yun S, Min J, Kim SJ and Kim J. DUSP1 induces paclitaxel resistance through the regulation of p-glycoprotein expression in human ovarian cancer cells. Biochem Bioph Res Commun 2016; 478: 403-409.
[58] Shen J, Li M and Min L. HSPB8 promotes cancer cell growth by activating the ERKCREB pathway and is indicative of a poor prognosis in gastric cancer patients. Oncol Rep 2018; 39: 2978-2986.

[59] Suzuki M, Matsushima-Nishiwaki R, Kuroyanagi G, Suzuki N, Takamatsu R, Furui T, Yoshimi N, Kozawa O and Morishige K. Regulation by heat shock protein 22 (HSPB8) of transforming growth factor-α-induced ovary cancer cell migration. Arch Biochem Biophys 2015; 571: 40-49.
[60] Teng F, Xu Z, Chen J, Zheng G, Zheng G, Lv H, Wang Y, Wang L and Cheng X. DUSP1 induces apatinib resistance by activating the MAPK pathway in gastric cancer. Oncol Rep 2018; 40: 1203-1222.
[61] Coca-Pelaz A, Rodrigo JP, Bradley PJ, Vander Poorten V, Triantafyllou A, Hunt JL, Strojan P, Rinaldo A, Haigentz M Jr, Takes RP, Mondin V, Teymoortash A, Thompson LD and Ferlito A. Adenoid cystic carcinoma of the head and neck-an update. Oral Oncol 2015; 51: 652-661.
[62] Qu J, Song M, Xie J, Huang X, Hu X, Gan R, Zhao Y, Lin L, Chen J, Lin X, Zheng D and Lu Y. Notch2 signaling contributes to cell growth, invasion, and migration in salivary adenoid cystic carcinoma. Mol Cell Biochem 2016; 411: 135-141.
[63] Ye X, He Y, Wang S, Wong GT, Irwin MG and Xia Z. Heart-type fatty acid binding protein (H-FABP) as a biomarker for acute myocardial injury and long-term post-ischemic prognosis. Acta Pharmacol Sin 2018; 39: 1155-1163.
[64] Lourenco SV, Kapas S, Williams DM, Leite K and Araujo VC. Expression patterns of integrins on pleomorphic adenoma and adenoid cystic carcinoma: study on specimens and in vitro investigation of the effects of extracellular matrix on the expression of these adhesion molecules. J Oral Pathol Med 2004; 33: 574-580.
[65] Shirasuna K, Saka M, Hayashido Y, Yoshioka H, Sugiura T and Matsuya T. Extracellular matrix production and degradation by adenoid cystic carcinoma cells: participation of plasminogen activator and its inhibitor in matrix degradation. Cancer Res 1993; 53: 147-152.
[66] Zboray K, Mohrherr J, Stiedl P, Pranz K, Wandruszka L, Grabner B, Eferl R, Moriggl R, Stoiber D, Sakamoto K, Wagner KU, Popper H, Casanova E and Moll HP. AKT3 drives adenoid cystic carcinoma development in salivary glands. Cancer Med 2018; 7: 445-453.
[67] Xie S, Yu X, Li Y, Ma H, Fan S, Chen W, Pan G, Wang W, Zhang H, Li J and Lin Z. Upregulation of lncRNA ADAMTS9-AS2 promotes salivary adenoid cystic carcinoma metastasis via PI3K/Akt and MEK/Erk signaling. Mol Ther 2018; 26: 2766-2778.
[68] Porta C, Paglino C and Mosca A. Targeting PI3K/Akt/mTOR signaling in cancer. Front Oncol 2014; 4: 64.
[69] Colak S and Ten Dijke P. Targeting TGF-β signaling in cancer. Trends Cancer 2017; 3: 56-71.
[70] Dong L, Wang YX, Li SL, Yu GY, Gan YH, Li D and Wang CY. TGF-beta1 promotes migration and invasion of salivary adenoid cystic carcinoma. J Dent Res 2011; 90: 804-809.
[71] Wang D, Chen X and Zhang R. BAMBI promotes macrophage proliferation and differentiation in gliomas. Mol Med Rep 2018; 17: 3960-3966.
[72] Natoni A, Macauley MS and O'Dwyer ME. Targeting selectins and their ligands in cancer. Front Oncol 2016; 6: 93.
[73] Rivera LB, Bradshaw AD and Brekken RA. The regulatory function of SPARC in vascular biology. Cell Mol Life Sci 2011; 68: 3165-3173.
[74] Tai IT and Tang MJ. SPARC in cancer biology: its role in cancer progression and potential for therapy. Drug Resist Update 2008; 11: 231-246.
[75] Ribeiro N, Sousa SR, Brekken RA and Monteiro FJ. Role of SPARC in bone remodeling and cancer-related bone metastasis. J Cell Biochem 2014; 115: 17-26.
[76] Kuo DS, Labelle-Dumais C and Gould DB. COL4A1 and COL4A2 mutations and disease: insights into pathogenic mechanisms and potential therapeutic targets. Hum Mol Genet 2012; 21: R97-R110.
[77] Lewis M. PRELP, collagen, and a theory of Hutchinson-Gilford progeria. Ageing Res Rev 2003; 2: 95-105.
[78] Hultgårdh-Nilsson A, Borén J and Chakravarti S. The small leucine-rich repeat proteoglycans in tissue repair and atherosclerosis. J Intern Med 2015; 278: 447-461.
[79] Fort A, Borel C, Migliavacca E, Antonarakis SE, Fish RJ and Neerman-Arbez M. Regulation of fibrinogen production by microRNAs. Blood 2010; 116: 2608-2615.
[80] Liu X, Zhang Y, Ren W, Cao T and Zhu Y. RNAi knockdown of C-erbB2 expression inhibits salivary gland adenoid cystic carcinoma SACC-83 cell growth in vitro. J Biomed Res 2010; 24: 215-222.
[81] Park S, Nam SJ, Keam B, Kim TM, Jeon YK, Lee S, Hah JH, Kwon T, Kim D, Sung M, Heo DS and Bang Y. VEGF and Ki-67 overexpression in predicting poor overall survival in adenoid cystic carcinoma. Cancer Res Treat 2016; 48: 518-526.
[82] Cerami E, Gao J, Dogrusoz U, Gross BE, Sumer SO, Aksoy BA, Jacobsen A, Byrne CJ, Heuer ML, Larsson E, Antipin Y, Reva B, Goldberg AP, Sander C and Schultz N. The cBio cancer genomics portal: an open platform for exploring multidimensional cancer genomics data: figure 1. Cancer Discov 2012; 2: 401-404.